Titre: Title:	Experimental study on the natural mixing behaviour of waste rocks poured in a paste backfill
Auteurs: Authors:	Yuyu Zhang, & Li Li
Date:	2023
Type:	Article de revue / Article
Référence: Citation:	Zhang, Y., & Li, L. (2023). Experimental study on the natural mixing behaviour of waste rocks poured in a paste backfill. International Journal of Mining, Reclamation and Environment, 25 pages. https://doi.org/10.1080/17480930.2023.2235847

Titre de la revue: Journal Title:	International Journal of Mining, Reclamation and Environment
Maison d'édition: Publisher:	Taylor & Francis
URL officiel: Official URL:	https://doi.org/10.1080/17480930.2023.2235847
Mention légale: Legal notice:	This is an original manuscript of an article published by Taylor & Francis in International Journal of Mining, Reclamation and Environment on 2023, available at: https://doi.org/10.1080/17480930.2023.2235847

Experimental study on the natural mixing behavior of waste rocks poured in a paste backfill

Yuyu Zhang[1*], and Li Li[2]

[1]Ph.D. Student

Research Institute of Mines and Environment (RIME UQAT-Polytechnique)

Department of Civil, Geological and Mining Engineering

Polytechnique Montréal

C.P. 6079, Succursale Centre-Ville, Montréal, Québec, Canada, H3C 3A7

E-mail: yuyu.zhang@polymtl.ca

[2]Full Professor, Ph.D.

Research Institute of Mines and Environment (RIME UQAT-Polytechnique)

Department of Civil, Geological and Mining Engineering

Polytechnique Montréal

C.P. 6079, Succursale Centre-Ville, Montréal, Québec, Canada, H3C 3A7

E-mail: li.li@polymtl.ca

[*]Corresponding author: Yuyu Zhang; E-mail: yuyu.zhang@polymtl.ca

Manuscript submitted to and accepted by: *International Journal of Mining, Reclamation and Environment*

[*] Corresponding author. E-mail: yuyu.zhang@polymtl.ca

Experimental study on the natural mixing behavior of waste rocks poured in a paste backfill

Abstract:

Underground produced waste rocks are typically hoisted and stored on ground surface as waste rock piles. The practice requires energy consumption for transporting the waste rocks from underground to ground surface and generates additional operation costs. An alternative practice is to directly pour the waste rocks into mine stopes being filled with paste backfill. However, the natural mixing behavior of waste rocks poured in a paste backfill has never been studied. To fill this gap, a series of physical model tests have been for the first time performed in the laboratory to understand the natural mixing behavior of waste rocks and paste backfill. The definitions of solids content by mass of waste rocks and mixing degree are for the first time proposed to quantitatively evaluate the mixing behavior between the poured waste rocks and paste backfill. The test results show that the penetration of waste rocks into paste backfill and mixing degree of poured waste rocks with paste backfill can be improved through the use of paste backfill of low solids content, large particle sizes of waste rocks, or/and through the increase of falling height of poured waste rocks. The proposed definitions of solids content by mass of waste rocks and mixing degree can be used as good indicators to quantitatively evaluate the mixing quality of the natural mixture.

Keywords: Underground mines; Mine backfill; Waste rocks; Paste backfill; Mixing degree; Natural mixture

1. Introduction

Underground mines produce a substantial amount of waste rocks during the development work in order to access ore bodies. Traditionally, these waste rocks need to be transported and hoisted to ground surface because there are no enough underground spaces for storing them. However, the transportation and haulage of waste rocks require large energy consumption and additional operation costs. The lack of enough trucks and haulage systems to transport waste rocks is another problem of this practice.

An alternative practice for industry is to directly pour the underground-produced waste rocks into mine stopes being filled with cemented paste backfill (main body) after the plug pour. These waste rocks are dumped into the cemented paste backfill at 1:1 ratio using a scoop right after excavation. No special crushing and sieving required before dumping. Once poured into paste backfill, the waste rocks mix with the cemented paste backfill in a natural way, without any need for mechanical mixing. This alternative practice can significantly reduce the energy consumption and operation costs associated with the hoisting and transportation of waste rocks from underground to ground surface (Lee & Gu 2017). In addition, if the waste rocks have a full mixing with the cemented paste backfill, the mixture can have mechanical properties much better than those of individual paste backfill and waste rocks (Qiu et al. 2020, 2022).

Despite these advantages, this practice also involves some risks. If the poured waste rocks are not fully mixed with the cemented paste backfill, the cohesionless waste rocks without any paste backfill may fail and collapse upon a side-exposure associated with the excavation of an adjacent stope. The failed mass could lead to ore dilution or even ore loss (Henning 2007). It is thus necessary to have a good understanding of the natural mixing behavior between the two materials.

However, almost all the existing studies related to backfills have been given on one single type of backfill, including the extensive works conducted by Li and other researchers (Aubertin et al. 2003; Béket Dalcé et al. 2019; El Mkadmi et al. 2014; Jaouhar et al. 2018; Jaouhar & Li 2019; Keita et al. 2021a, 2021b; Li et al. 2003; Li et al. 2005; Li & Aubertin 2012; Li 2014a, 2014b; Li & Aubertin 2014; Liu et al. 2017a, 2017b, 2018; Pagé et al. 2019; Qin et al. 2021a, 2021b; Sobhi et al. 2017; Sobhi & Li 2017; Wang et al. 2021a, 2021b; Wang & Li 2022; Yan et al. 2020; Yan et al. 2022a, 2022b; Yang et al. 2017, 2018; Zhai et al. 2021; Zheng & Li 2020; Zheng et al. 2019, 2020a, 2020b, 2020c).

One can only see a few publications related to the mixtures of graded waste rocks and tailings (Wickland & Wilson 2005; Wilson 2001; Wilson et al. 2008) or the graded waste rocks and cemented hydraulic fill (Kuganathan & Sheppard 2001). The abovementioned mixtures require the waste rocks and tailings or hydraulic fill to be mechanically mixed in pipes or special mixing machines. Crushing and sieving are also necessary to limit the sizes of waste rocks. These mechanical mixtures are thus completely different from the natural mixture of waste rocks poured in a paste backfill. Recently, Veenstra & Grobler (2021) present a concept, by which a waste rocks structure is built and wrapped by cemented paste backfill. It can also allow the maximum use of waste rocks and avoid the transportation and hoist of waste rocks from underground to ground surface. However, they do not show how the poured waste rocks are mixed with the paste backfill in a stope.

Until now, the study on the natural mixing behavior of waste rocks poured in a paste backfill is absent. To fill this gap, in this paper, a series of physical model tests have been for the first time performed in laboratory to show the natural mixing behavior of waste and paste backfill. The definitions of solids content by mass of waste rocks and mixing degree are proposed for the first time to quantitatively describe the natural mixture between waste rocks and paste backfill. The effects of some key influencing factors on the natural mixing behavior between the two materials are investigated and discussed.

2. Laboratory tests

2.1. Materials

In this study, an uncemented paste backfill made of full tailings was used to facilitate the investigation of the natural mixing behavior between the waste rocks and paste backfill. The tested tailings were taken from a mine located at the northwest of Québec, Canada. Fig. 1 illustrates the particle size distribution curve of the tailings. It has a maximum particle size of 0.63 mm, containing approximately 77% of particles smaller than 80 µm and 36% smaller than 20 µm. The backfill made of such tailings meets the criterion of paste backfill in terms of particle size distribution (contains at least 15% of particle smaller than 20 µm) (Hassani & Archibald 1998; Potvin et al. 2005; Zheng & Li 2020).

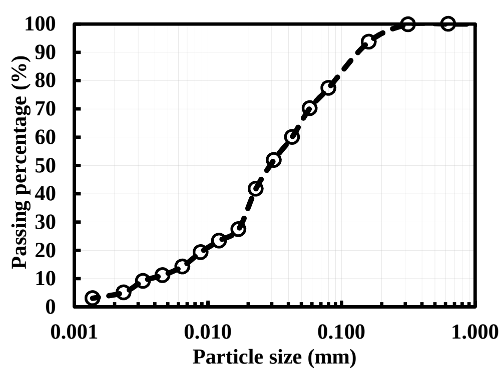

Fig. 1 Particle size distribution curve of the tested tailings

The tested tailings were first dried in an oven for 24 hours. The dried tailings were then poured into water to make a paste backfill (Fig. 2a). A full mixing between the tailings and water was guaranteed by the use of an electric stirring rod, as shown in Fig. 2b.

(a) (b)

Fig. 2 Procedures for making a homogenous paste backfill: (a) addition of dried tailings into water; (b) mixing with an electric stirring rod

The tested paste backfills were prepared with three solids contents by mass of 70, 72.5, and 75%, respectively. With a solids content by mass of 70%, the paste backfill looks like a liquid, as shown in Fig. 3a. At a solids content by mass of 72.5%, the paste backfill still looks like a liquid (Fig. 3b), but much thicker than the previous paste backfill with a solids content by mass of 70%. At a solids content by mass of 75%, the paste backfill becomes thick and viscous, looking like a paste (Fig. 3c).

(a) (b) (c)

Fig. 3 Pictures of paste backfills having solids contents by mass of: (a) 70%, (b) 72.5%, and (c) 75%, respectively

The tested waste rocks were taken from the same mine from where the tailings were taken. Sieving was performed to obtain waste rocks samples with particle sizes in the range of 2.5 to 5.0, 5.0 to 8.0, and 8.0 to 9.5 mm, as shown in Fig.4. They were named as small, medium and large particle size waste rocks samples, and tinted of blue (Fig. 5a), green (Fig. 5b) and yellow (Fig. 5c) colors, respectively. The coloring of waste rocks samples is necessary to better observe the mixing state between waste rocks and paste backfill after cutting the backfill mass formed by pouring the waste rocks into the paste backfill.

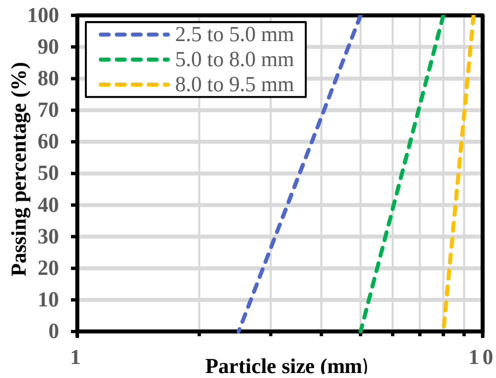

Fig. 4 Particle size distribution curves of the tested waste rocks

(a) (b) (c)

Fig. 5 Tinted waste rocks samples with different particle sizes: (a) small particle sizes in the range of 2.5 to 5.0 mm; (b) medium particle sizes in the range of 5.0 to 8.0 mm; (c) large particle sizes in the range of 8.0 to 9.5 mm

2.2. Testing procedure

Fig. 6 shows a schematic presentation (Fig. 6a) and a picture (Fig. 6b) of the physical model, used to study the natural mixing behavior of waste rocks poured in a paste backfill. On Fig. 6a, H_{paste} represents the height of the paste backfill before any pouring of waste rocks; P is the solids content by mass of paste backfill; H_f is the falling height of waste rocks. The box of 16.5 cm long, 20 cm large and 25 cm high was used to simulate an underground mine stope in reduced scale (see Fig. 6b). It is made of wood studs to ease the later box disassembling and sample cut. Its inside walls were covered with waterproof plastic sheet to prevent any water seepage. A funnel was fixed at the top center of the mold to control the falling height, position of pouring, and quantity of waste rocks. The funnel has a diameter of 19 cm on top, a diameter of 4.0 cm at the end with the exit tube, and an overall height of 12 cm. In this study, the tested waste rocks were poured through the funnel at the center area of the mold. All tests were done by using a total mass of waste rocks M_{wr} = 1000 g and an initial height of paste backfill H_{paste} = 10 cm. In this study, no plug is poured into the mold before the pouring of paste backfill.

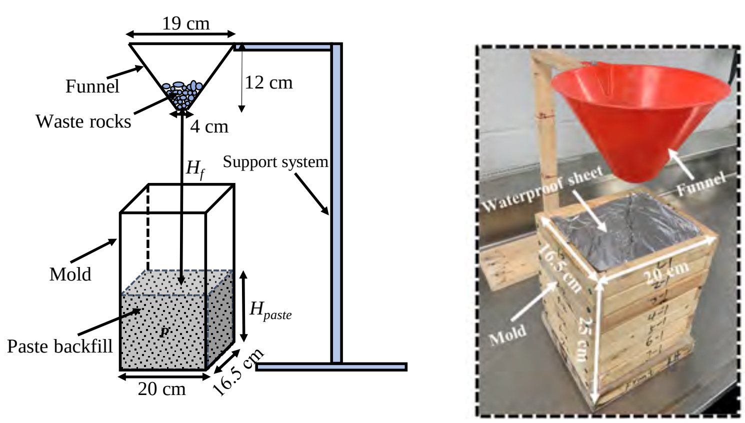

(a) (b)

Fig. 6 A physical model to study the natural mixing behavior of waste rocks poured in a paste backfill: (a) schematic presentation; (b) a picture

Table 1 shows the test program to evaluate the effects of solids content by mass (P) of paste backfill, particle sizes (d_{wr}) of waste rocks and falling height (H_f) of waste rocks on the natural mixing behavior between the two materials.

Table 1 Test program of natural mixing between waste rocks and paste backfill

Cases	d_{wr} (mm)	H_f (cm)	P (%)
Case 1	2.5 to 5.0	15	70
Case 2	2.5 to 5.0	15	72.5
Case 3	2.5 to 5.0	15	75
Case 4	5.0 to 8.0	15	72.5
Case 5	8.0 to 9.5	15	72.5
Case 6	2.5 to 5.0	45	72.5
Case 7	2.5 to 5.0	75	72.5

After the pouring of waste rocks into the paste backfill, the natural mixture was left to settle down and dry. When it became hard enough, the wood studs were disassembled with the mixture was then cut into small blocks. Fig. 7 shows the schematic presentation of the cut procedure of a mixture. The mixture was divided into three layers along the Z direction. Each layer was further cut into 12 small blocks of 5.5 cm long, 5 cm large and 3 cm high. The position of each small block is identified by its layer number along with Z direction and its numbers in X and Y directions.

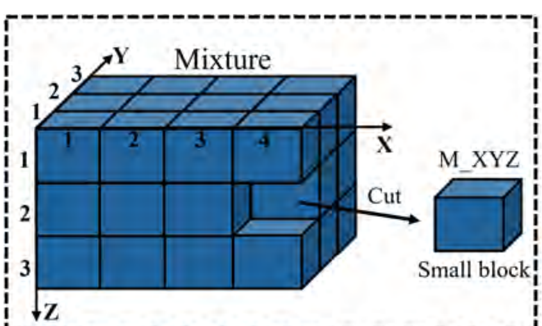

Fig. 7 Schematic presentation of the cut procedure of the mixture

The obtained small blocks were then placed in an oven to make them completely dried. After 24 hours of drying, each block was gently crushed by hand and placed in a container, followed by a sieving analysis. The masses of waste rocks and paste backfill of each block were then obtained due to the large contrast in particle size distribution between the tested waste rocks and paste backfill. These steps are illustrated in Fig. 8 showing the state of dried blocks (Fig. 8a), a crushed block (Fig. 8b), and sieving analysis (Fig. 8c), respectively.

(a) (b) (c)

Fig. 8 Procedure for obtaining the particle size distribution curves of a small block: (a) small blocks after 24 hours of oven-drying; (b) hand-crushed mixture of a dried block; (c) sieving analysis

3. Test results and interpretation

3.1. Qualitative analysis

3.1.1 Effect of the solids content by mass of paste backfill

Fig. 9 presents a top view of the mixtures after the pour of small particle size of waste rocks in the paste backfills having three different solids contents by mass of 70 (Case 1), 72.5 (Case 2), and 75% (Case 3), respectively (see Table 1 for more details). At a solids content by mass of 70%, the waste rocks easily penetrated into the paste backfill and almost all the poured waste rocks sunk into the paste backfill with only a few tracks left on the top surface of the mixture (Fig. 9a). At a solids content by mass of 72.5%, the penetration of waste rocks into the paste backfill became difficult and the drag force against the sinking of waste rocks particles would be stronger than in the paste backfill of 70%. Subsequently, a large amount of waste rocks remained on the top surface without mixing with any paste backfill (Fig. 9b). When the solids content of the paste backfill further increases to 75%, the waste rocks are difficult to penetrate into and sink in the paste backfill. Accordingly, the major part of the poured waste rocks remained on the top surface of the mixture (Fig. 9c).

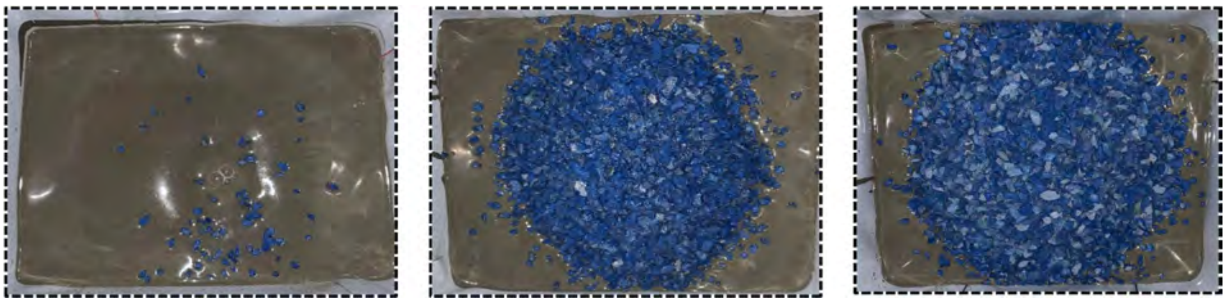

(a) (b) (c)

Fig. 9 Top views of the mixtures after the pour of waste rocks in the paste backfills having solids contents by mass of: (a) 70% (Case 1); (b) 72.5% (Case 2); (c) 75% (Case 3)

Fig. 10 presents the views of the internal structures of the mixtures between the poured small particle size waste rocks and the paste backfills having a solids content by mass of 70% (Fig. 10a), 72.5% (Fig. 10b), and 75% (Fig. 10c), respectively. With a solids content of 70%, one sees the presence of waste rocks along the whole depth with all the particles entirely wrapped of paste backfill (Fig.10a). The mixture between the waste rocks and paste backfill has a texture looking like a concrete. When the solids content increases to 72.5%, one sees a large pocket of waste rocks along the depth of 0 to 3 cm in the form of an inverse cone or a volcano crater without any mix with paste backfill (Fig. 10b). Along the depth of 3 to 9 cm, one sees the presence of waste rocks entirely wrapped of paste backfill, indicating a good mixture. At a solids content of 75%, one can see the waste rocks also in the form of an inverse cone or volcano crater along the depth of 0 to 3 cm. No waste rocks submerged into the paste backfill along the depth of 3 to 9 cm (Fig. 10c). The results along with those presented in Fig. 9 indicate that a good mixture between poured waste rocks and paste backfill exists only when the paste backfill has a low solids content. When the solids content of paste backfill is high, the quantity of unmixed waste rocks increases. The mixing behavior between the poured waste rocks and paste backfill varies in space (depth).

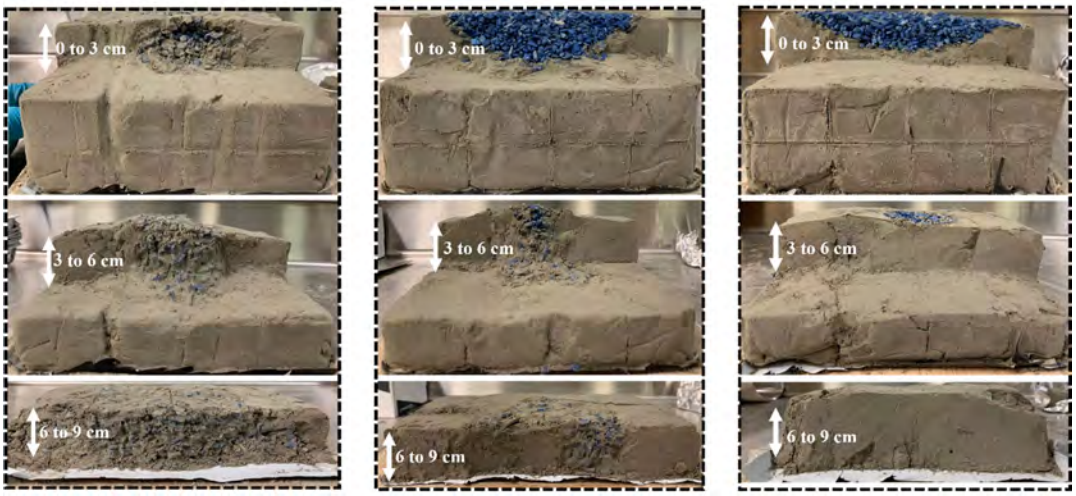

(a) (b) (c)

Fig. 10 Internal structures of the mixtures after the pour of waste rocks in the paste backfills having solids contents by mass of: (a) 70% (Case 1); (b) 72.5% (Case 2); (c) 75% (Case 3)

Fig. 11 presents the particle size distribution (PSD) curves of the tested tailings and waste rocks (WR) along with the PSD of the small blocks issued from the cut of mixture generated by pouring small particle size waste rocks into paste backfills having a solids content by mass of 70 (Fig. 11a), 72.5 (Fig. 11b) and 75% (Fig. 11c), respectively. At a solids content by mass of 70% (Fig. 11a), the mass of paste backfill for each block increases as the increase of mixture depths (from Layer 1 to 3). The high amount of paste backfill in each block indicates the waste rocks are well mixed with paste backfill. When the solids content by mass of paste backfill increase to 72.5% (Fig. 11b), the PSD curves of the two center blocks (M_221 and M_321) at layer 1 overlap with the PSD curve of waste rocks, indicating an absence of paste backfill in the blocks. At a solids content by mass of 75% (Fig. 11c), the PSD curves of two center blocks (M_221 and M_321) at layer 1 also overlap with that of waste rocks, once again indicating an absence of paste backfill in these blocks. These results confirm that, for a given mass, particle sizes and falling height of waste rocks, the quantity of unmixed waste rocks can be expected to increase as the solids content of paste backfill increases.

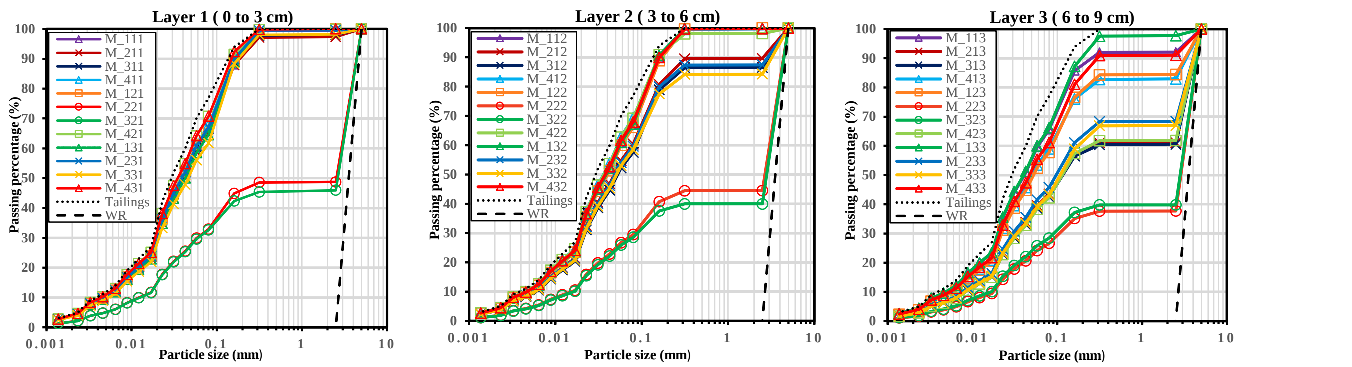

(a)

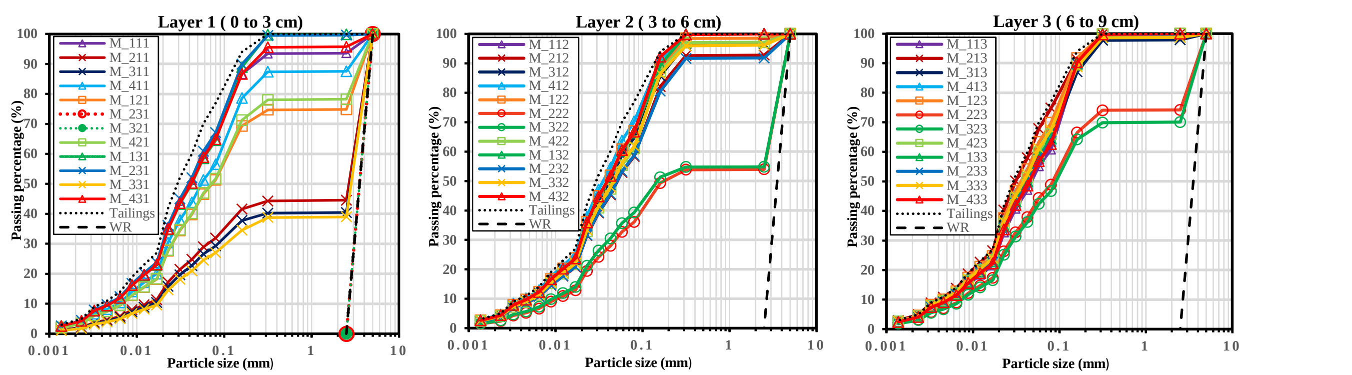

(b)

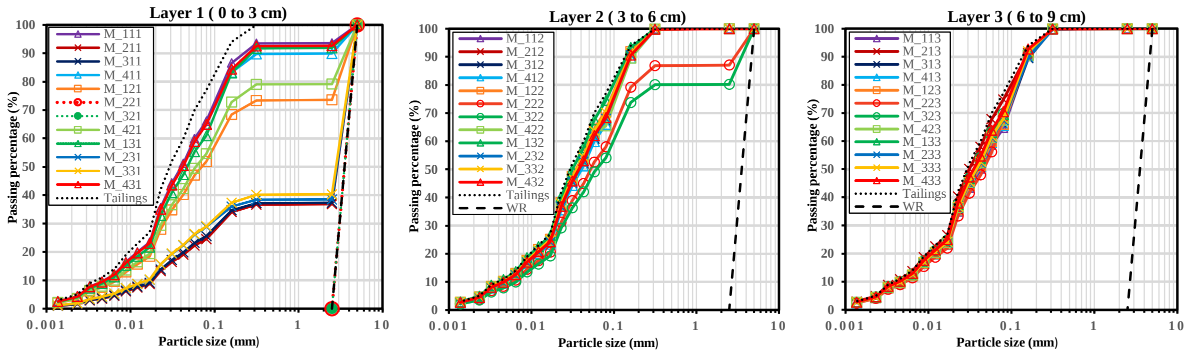

(c)

Fig. 11 Particle size distribution (PSD) curves of small blocks after the pour of waste rocks in the paste backfills having solids contents by mass of: (a) 70% (Case 1); (b) 72.5% (Case 2); (c) 75% (Case 3)

3.1.2 Effect of the particle size of waste rocks

Fig. 12 presents the top views of the mixtures after the pour of small particle sizes waste rocks (Case 2), medium particle sizes waste rocks (Case 4) and large particle sizes waste rocks (Case 5) in the paste backfills having a solids content by mass of 72.5%, respectively. One sees that a large quantity of waste rocks stayed on the top surface for the case of small particle size waste rocks (Fig. 12a), while only a small portion of waste rocks remained on the top surface for the case of large particle size waste rocks (Fig. 12c). With the medium particle size waste rocks, a quantity intermediate between the two previous cases were observed on the top surface of the mixture (Fig. 12b). These results indicate that large particle sizes of waste rocks are preferred in terms of penetration of poured waste rocks in a given paste backfill.

(a) (b) (c)

Fig. 12 Top views of the mixtures after the pour of waste rocks with: (a) small particle sizes (Case 2); (b) medium particle sizes (Case 4); (c) large particle sizes (Case 5)

Fig. 13 presents the internal structures of the mixtures after the pouring of waste rocks with small particle sizes waste rocks (Fig. 13a), medium particle sizes waste rocks (Fig. 13b) and large particle sizes waste rocks (Fig. 13c), exposed after a few vertical cuts. In all cases, the waste rocks were poorly mixed with paste backfill in the center part of the paste backfill along the depth of 0 to 3 cm, while the waste rocks are all wrapped by paste backfill along the depth of 3 to 9 cm.

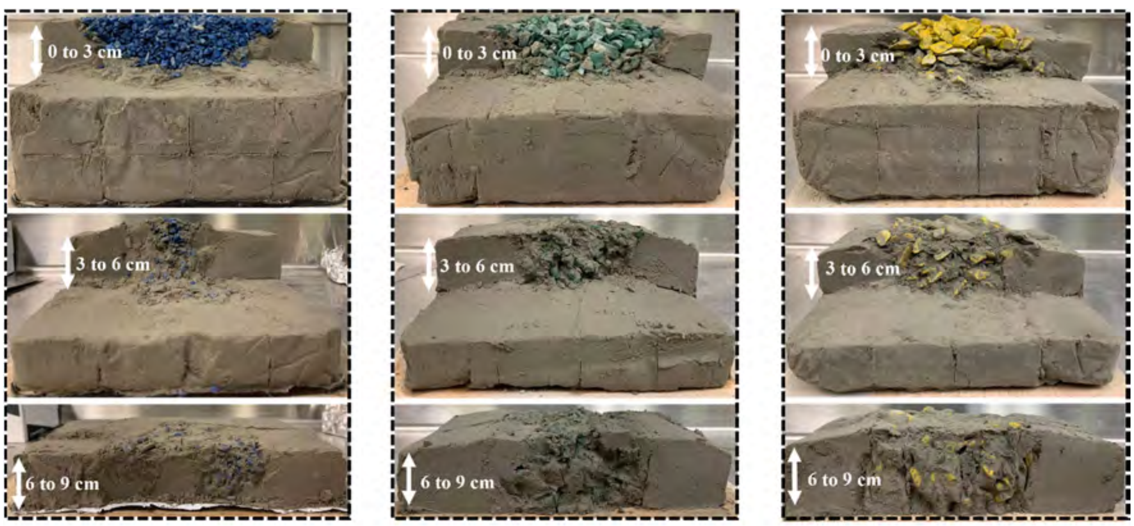

(a) (b) (c)

Fig. 13 Internal structures of the mixtures after the pour of waste rocks with: (a) small particle sizes (Case 2); (b) medium particle sizes (Case 4); (c) large particle sizes (Case 5)

The PSD curves of small blocks after the pour of waste rocks with small particle sizes has already been presented in Fig. 11b (Case 2). Fig. 14 only presents the PSD curves of small blocks after the pour of waste rocks with medium particle sizes (Fig. 14a) and large particle sizes (Fig. 14b), respectively. For waste rocks with medium particle sizes (Fig. 14a), the two center blocks at layer

1 (M_221 and M_321) contain 8.7 and 5.6% of paste backfill, respectively, suggesting a little presence of paste backfill in these blocks. For waste rocks with large particle sizes (Fig. 14b), the mass of paste backfill at the corresponding two center blocks increases to 16.5 and 13.1 %, respectively. The PSD curves of other blocks for waste rocks with medium and large sizes are similar. These results suggest that, for paste backfill with a high solids content, the increase of waste rocks particle sizes can help to improve the mixing behavior between the two materials.

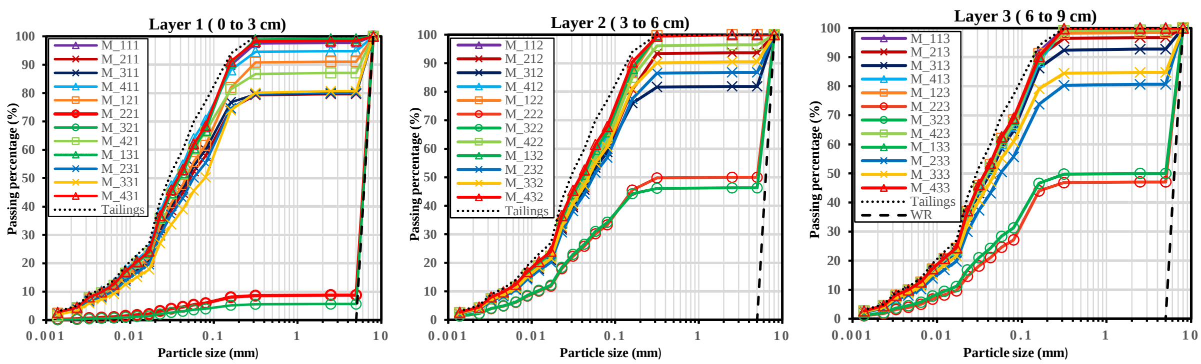

(a)

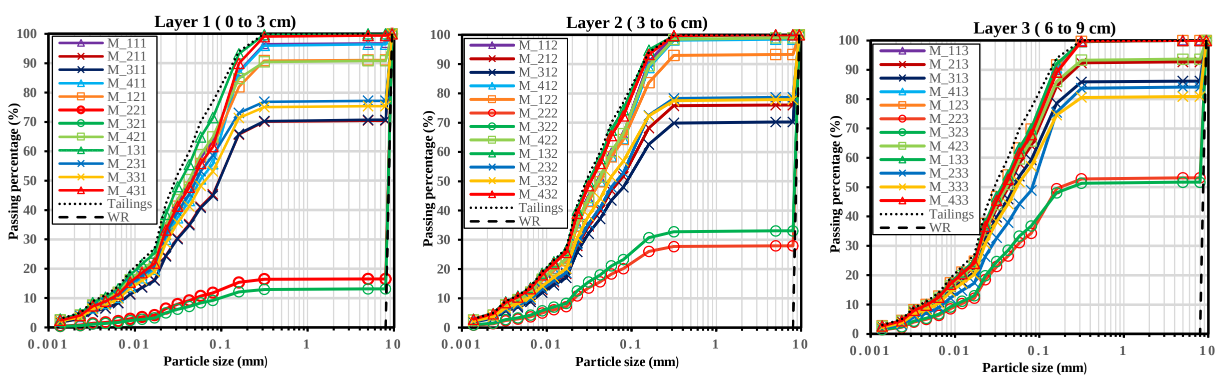

(b)

Fig. 14 Particle size distribution (PSD) curves of small blocks after the pour of waste rocks with: (a) medium particle sizes of 5.0 to 8.0 mm (Case 4); (b) large particle sizes of 8.0 to 9.5 mm (Case 5)

3.1.3 Effect of the falling height of waste rocks

Fig. 15 presents the top views of the mixtures after the pour of waste rocks in the paste backfill having a solids content by mass of 72.5% at falling heights of 15 (Case 2), 45 (Case 6) and 75 cm (Case 7), respectively. One sees a large amount of waste rocks remaining on the top surface of the mixture at a falling height of 15 cm (Fig. 15a). The mass of waste rocks on the top surface of the mixture decreases with the falling height increases to 45 cm (Fig. 15b). When the falling height further increases to 75 cm, almost all the waste rocks sunk into the paste backfill, resulting in a very small quantity of waste rocks particles on the top surface of the mixture (Fig. 15c).

(a) (b) (c)

Fig. 15 Top views of the mixtures after the pour of waste rocks in the paste backfills having a solids content by mass of 72.5% at falling heights of: (a) 15 cm (Case 2); (b) 45 cm (Case 6); (c) 75 cm (Case 7)

Fig. 16 presents the internal structures of the mixtures after the pouring of waste rocks at falling heights of 15 (Fig. 16a), 45 (Fig. 16b) and 75 cm (Fig. 16c), respectively. From Fig. 16a, one notes that the quantity of submerged waste rocks inside the paste backfill are small when the waste rocks are poured at the falling height of 15 cm. However, the quantity of submerged waste rocks increase as the falling heights increases to 45 cm (Fig. 16b). All the waste rocks are submerged into the paste backfill as the falling heights increases to 75 cm (Fig. 16c). The submerged waste rocks are entirely wrapped by the paste backfill, suggesting a good mixture.

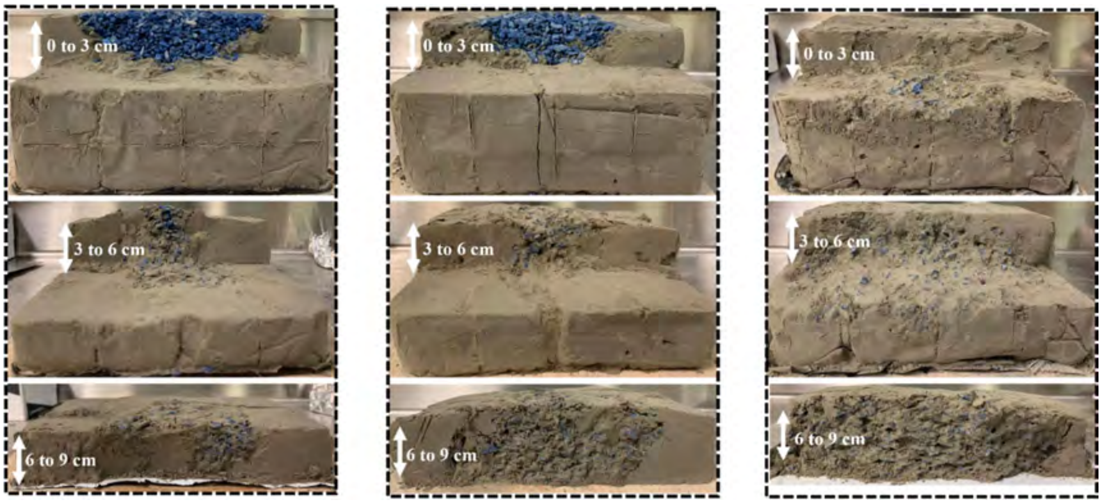

(b) (b) (c)

Fig. 16 Internal structures of the mixtures after the pour of waste rocks at falling heights of: (a) 15 cm (Case 2); (b) 45 cm (Case 6); (c) 75 cm (Case 7)

The PSD curves of small blocks after the pour of waste rocks at the falling height of 15 cm has been shown in Fig. 11b (Case 2). Fig. 17 presents the PSD curves of small blocks after the pour of waste rocks at falling heights of 45 (Fig. 17a) and 75 cm (Fig. 17b), respectively. At a falling height of 45 cm, one sees that the center blocks at layer 1 (M_221 and M_321) contain around 19.1%, suggesting a little amount of paste backfill in these blocks. At a falling height of 75 cm, the two center blocks at layer 1 (M_221 and M_321) contain about 80% of paste backfill, indicating the presence of large quantity of paste backfill. The results along with the findings of falling height at 15 cm (Fig. 11b) indicate, for paste backfill with a high viscosity, the mixing behavior between the two materials can be improved by increasing the falling height of waste rocks.

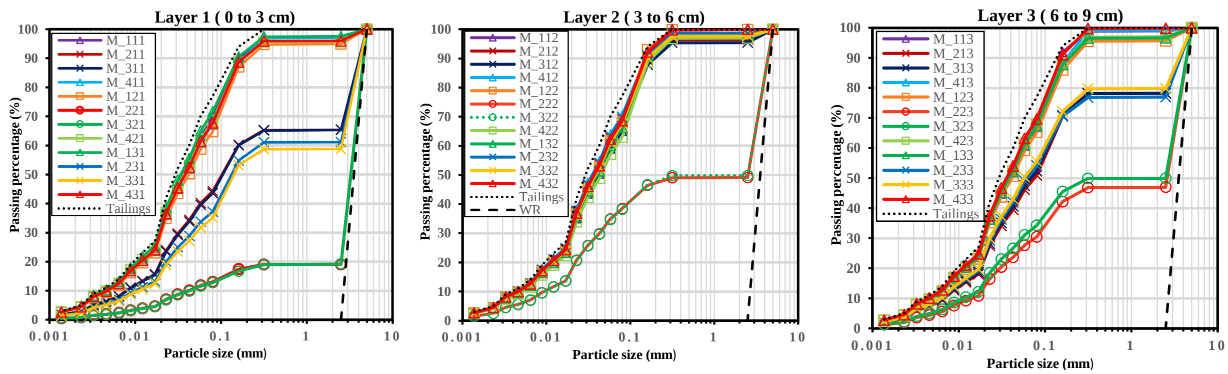

(a)

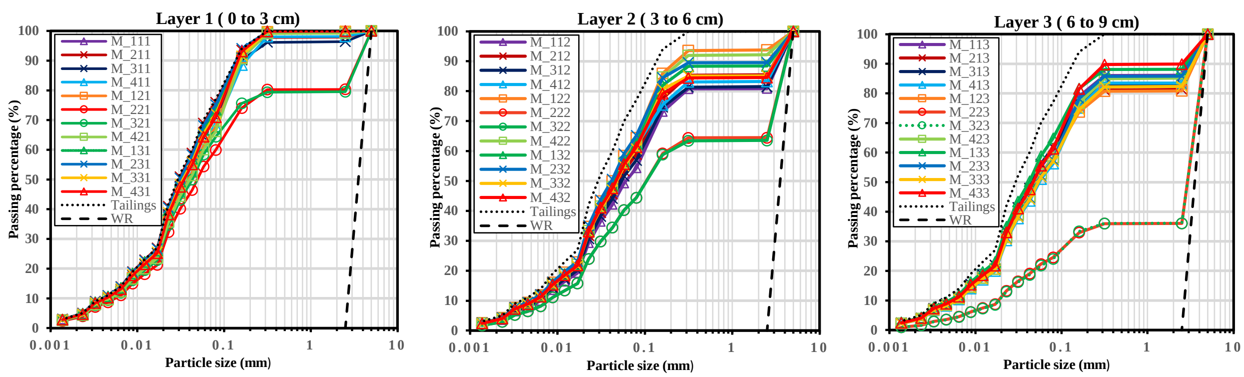

(b)

Fig. 17 Particle size distribution (PSD) curves of small blocks after the pour of waste rocks at falling heights of: (a) 45 cm (Case 6); (b) 75 cm (Case 7)

3.2. Spatial distribution of mixing degree between waste rocks and paste backfill

In section 3.1, the mixing behavior between the poured waste rocks and paste backfill has been presented in a qualitative way. It gave a global and general picture of the internal structure of a mixture. However, it does not allow a quantitative description on the mixing degree of mixture or a spatial description on the mixing degree of the mixture between the two materials. To overcome these limitations, one first needs the definition of a parameter that can be used to quantitatively evaluate the degree of mixture between two different materials. As such definition is absent in the literature, one first proses a definition of waste rocks content by mass as follows:

$$C = \frac{M_{wr}}{M_{wr} + M_{paste.dried}} \tag{1}$$

where C is the solids content by mass of waste rocks of a mixture, M_{wr} and M_{paste} are the masses of waste rocks and dried paste backfill in the mixture, respectively. When $M_{wr} = 0$, the mixture does not contain any waste rocks and the solids content by mass of waste rocks C is equal to 0%. When $M_{paste.dried} = 0$, the mixture does not contain any paste backfill and the solids content by mass of waste rocks C is equal to 100%.

The solids content by mass of waste rocks can give an idea on the portion of waste rocks, but fail to describe the mixing degree between paste backfill and waste rocks. If one considers that a full mixture between the two materials is reached when the voids of waste rocks are fully filled with paste backfill. The mixing degree of the mixture between the two materials can be defined as follows:

$$S = \frac{V_{paste.dried}}{V_v} \tag{2}$$

where S is the mixing degree of a mixture, $V_{paste.dried}$ is the volume of dried paste backfill in a mixture, V_v is the voids volume of waste rocks.

The volume of dried paste backfill in a mixture can then be obtained by:

$$V_{paste.dried} = \frac{M_{paste.dried}}{\rho_{paste.dried}} \tag{3}$$

where $M_{paste.dried}$ is the mass of dried paste backfill in a mixture; $\rho_{paste.dried}$ is the density of dried paste backfill in a mixture, defined as follows:

$$\rho_{paste.dried} = \rho_s * (1 - n_{paste.dried}) \tag{4}$$

where ρ_s is the particle density of tailings particles; $n_{paste.dried}$ is the porosity of dried paste backfill, expressed as:

$$n_{paste.dried} = \frac{e_f}{1 + e_f} \tag{5}$$

where e_f is the final void ratio of dried paste backfill determined from shrinkage test curve (Qin et al. 2021b; Saleh-Memba et al. 2016).

The voids volume of waste rocks in a mixture can be obtained by:

$$V_v = V_{wr} * n_{wr} \tag{6}$$

where V_v is the voids volume of waste rocks, n_{wr} is the porosity of waste rocks; V_{wr} is the volume of waste rocks, obtained as follows:

$$V_{wr} = \frac{M_{wr}}{\rho_{wr}} \tag{7}$$

where M_{wr} is the mass of waste rocks in a mixture, ρ_{wr} is the density of waste rocks.

Substituting equations (3) to (7) into equation 2, the mixing degree of a mixture becomes:

$$S = \frac{M_{paste.dried} * \rho_{wr}}{\rho_s \left(1 - \frac{e_f}{1 + e_f}\right) * M_{wr} * n_{wr}} \tag{8}$$

If the mass of dried paste backfill, $M_{paste.dried}$ equals to zero, the mixing degree of the mixture, *S*, equals to zero. The mixing degree of the mixture increases as the mass of dried paste backfill of the mixture increases. When the mass of paste backfill increases to a degree by which all the void volume of waste rocks is filled with paste backfill, the mixing degree of the mixture, *S*, equals to 100%. If the mass of paste backfill increases further, the void volume and porosity of the waste rocks increase. Equation (8) cannot be applied by considering n_{wr} as a constant. The mixing degree of the mixture can either be considered as 100% or inapplicable.

Figs. 18 and 19 respectively shows the spatial distributions of solids contents by mass of waste rocks C and mixing degree S of the mixtures for Cases 1 to 7. Details on the direct measurements and calculations of the solids content by mass of waste rocks and mixing degree for each small block are presented in Appendix I, while the correction and estimation of the solids content by mass of waste rocks and mixing degree of the mixture for the small blocks near the interfaces between waste rocks and paste backfill are presented in Appendix II.

From Fig. 18, one sees the solids content by mass of waste rocks varies from 50 to 60% inside the center area of the mixture (Case 1), suggesting most waste rocks are presented in these areas. For Cases 2, 3, 4 and 6, the solids content by mass of waste rocks ranges from 90 to 100% on the top part of the mixtures, indicating a high amount of waste rocks with the absence of paste backfill in these areas. One can find that the spatial distributions of the solids contents by mass of waste rocks agree well with the observations and qualitative analyses shown in Figs. 9 to 17. The solids content by mass of waste rocks can give a quantitative description on the portion of waste rocks for each of the mixture, thus can be used as an indicator to describe the mixing behavior of the mixture.

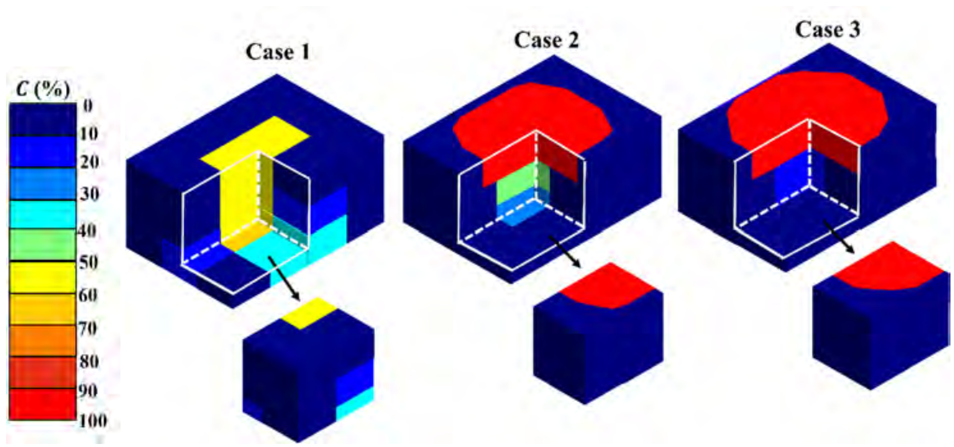

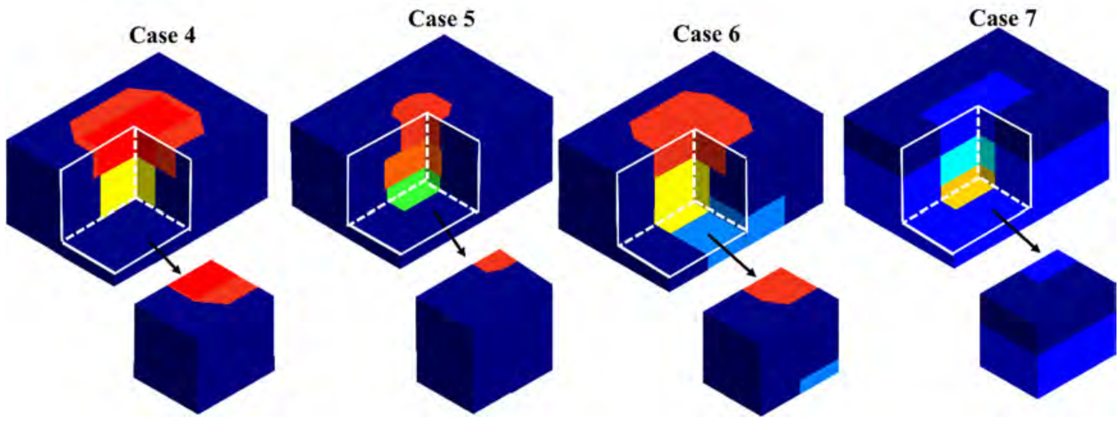

Fig. 18 The spatial distributions of solids content by mass of waste rocks C for Cases 1 to 7

Fig. 19 shows that the spatial mixing quality between the poured waste rocks and paste backfill of a mixture is presented in a quantitative way. For Cases 1 and 7, the mixing degree of the mixtures equals to 100%, indicating the waste rocks are fully mixed with the paste backfill. For Cases 2, 3 and 4, the mixing degree on the top part of the mixtures vary from 0 to 20%, suggesting the waste rocks are poorly mixed with the paste backfill in these areas. For Cases 5 and 6, the mixing degree on the top ranges from 30 to 50%, which also confirms the waste rocks are not fully mixed with the paste backfill. The mixing degree reaches 100% at the bottom parts of the mixtures for all cases.

Both figures indicate that the portions of pure waste rocks can be decreased by using paste backfill of low solids content, waste rocks of large particle sizes and large falling height. The proposed definition of solids content by mass of waste rocks C and mixing degree S can be used to quantitatively describe the natural mixing behavior between poured waste rocks and paste backfill.

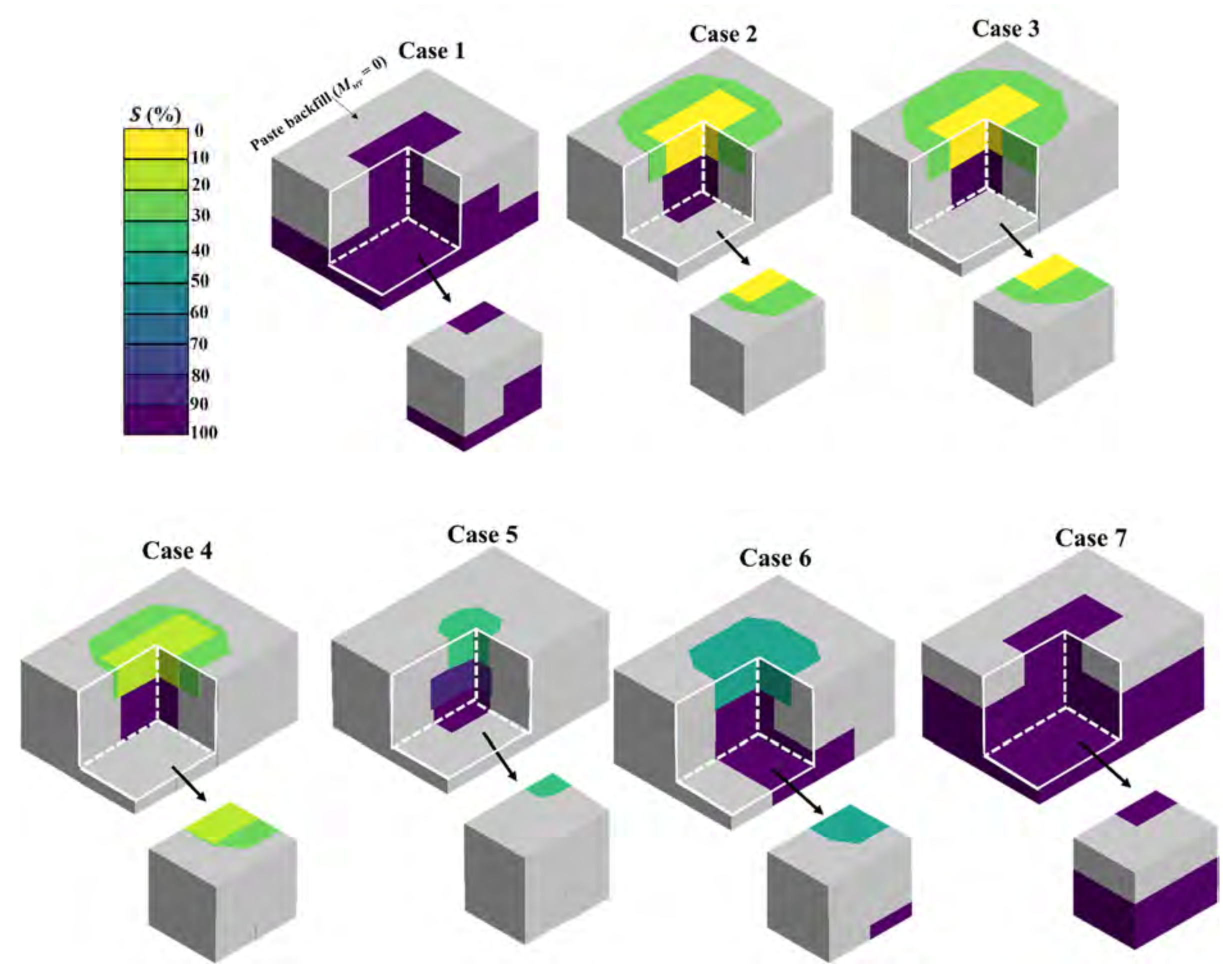

Fig. 19 The spatial distributions of mixing degree *S* for Cases 1 to 7

4. Discussion

A series of physical model tests were performed to investigate the natural mixing behavior of waste rocks poured in a paste backfills. The effects of solids content of paste backfill, particle size of waste rocks, and falling height of waste rocks on the natural mixing behavior of poured waste rocks and paste backfill is for the first time evaluated. Two definitions used to quantitatively describe the nature mixing behavior of waste rocks and paste backfill were also proposed for the first time. The test results can be used to understand the natural mixing behavior of poured waste rocks with a paste backfill in a mine stope.

Nevertheless, it should be noted that the experimental work presented in this study is preliminary and involves several limitations. As a very preliminary stage without any references (neither in published works nor for a specific mine or stope), the solids contents of paste backfill, sizes and falling height of waste rocks, and box sizes were chosen in an arbitrary way. No scale factors can be considered because the on-site conditions are unknown. In the future, more experimental and field works are necessary by considering the scale effect factors. The use of non-cemented paste backfill constitutes another limitation of the test program presented in Table 1. The effect of binder on the natural mixing behavior of waste rocks and cemented paste backfill will be investigated in the following works. More experimental tests will also be conducted to obtain the rheology parameters (e.g., viscosity and yield stress) used to describe the flowability of cemented paste backfill. These are part of our ongoing works and will be part of our future publications.

In the study, the mass of waste rocks was used as a control variable for the sake of simplicity in laboratory tests. However, volume of waste rocks is a better variable than mass of waste rocks because it allows to consider the capacity of paste backfill holding the waste rocks. The control variable of waste rocks volume will be applied in the future works. In addition, the waste rocks were poured into the paste backfill from the top center of the mold. This does not always correspond to the field conditions where waste rocks are commonly dumped in a stope being filled with waste rocks from an over-cut at a stope edge. More experimental work is thus necessary to investigate the effect of pouring position on the mixing behavior between poured waste rocks and paste backfill.

Another limitation of this study is associated with the cut size of small block. The same size was used for all the small blocks. This results in inaccurate descriptions of the solids content by mass of waste rocks and mixing degree of the mixture, especially near the interfaces between waste rocks and paste backfill. In future studies, the blocks around the interfaces between waste rocks and paste backfill should be cut in dimensions as small as possible to obtain a more accurate description of the mixing degree between the two materials.

Despite the above-mentioned limitations, the experimental results and the analyses presented in this study result in a better understanding of the natural mixing behavior between the poured waste rocks and paste backfill. The results along with the proposed definitions of solids content by mass of waste rocks and mixing degree of the mixture of this study pave the way for future work on the natural mixing behavior of waste rocks and paste backfill.

5. Conclusions

In this study, the natural mixing behavior of waste rocks poured in a paste backfill has been, for the first time, investigated through laboratory tests. The definitions of solids content by mass of waste rocks and mixing degree of mixtures were for the first time proposed to quantitatively describe the mixture between the poured waste rocks and paste backfill. The main findings are summarized as follows:

1. For a given mass, particle sizes and falling height of waste rocks, the quantity of unmixed waste rocks can be expected to increase as the solids content of paste backfill increases.
2. The mixing behavior between the poured waste rocks and paste backfill varies in space of a mixture.
3. The mixing degree of poured waste rocks and paste backfill can be improved through the use of paste backfill of low solids content, large particle sizes of waste rocks, or through the increase of falling height of poured waste rocks.

4. The proposed definitions of solids content by mass of waste rocks and mixing degree of the mixtures seem to be appropriate describe the spatial mixing behavior of the waste rocks and paste backfill. They can be used as good indicators to quantitatively evaluate the mixing quality of the natural mixture.

Acknowledgments

The authors acknowledge the financial support from the Natural Sciences and Engineering Research Council of Canada (NSERC RGPIN-2018-06902), Natural Sciences and Engineering Research Council of Canada (NSERC ALLRP 580767 - 22), Fonds de recherche du Québec – Nature et technologies (FRQNT 2017-MI-202860), Mitacs Elevate Postdoctoral Fellowship (IT12569), and industrial partners of the Research Institute on Mines and the Environment (RIME UQAT – Polytechnique; http://rime-irme.ca).

Appendix I: Solids content by mass of waste rocks *C* and mixing degree *S* of the small blocks

Table A1 presents the solids content by mass of waste rocks and mixing degree of the mixtures using the proposed equations (1) and (8) . In the calculations, the final void ratio e_f of dried paste backfill is determined by using the shrinkage test results conducted by Saleh-Memba et al. (2016).

Table A1 Calculated solids content by mass of waste rocks *C* and mixing degree *S* of small blocks based on direct measurements

Case 1	Blocks	M_{wr}(kg)	$M_{paste.dried}$(kg)	ρ_s (kg/m^3)	e_f	C	S
Layer 1	M_111	0.0007	0.1267	2710	0.6	0.55%	/
	M_211	0.0027	0.0985	2710	0.6	2.67%	/
	M_311	0.0020	0.0967	2710	0.6	2.03%	/
	M_411	0.0000	0.1255	2710	0.6	0.00%	/

	M_121	0.0000	0.1052	2710	0.6	0.00%	/
	M_221	0.0673	0.0639	2710	0.6	51.30%	100.0%
	M_321	0.0479	0.0407	2710	0.6	54.06%	100.0%
	M_421	0.0001	0.1057	2710	0.6	0.09%	/
	M_131	0.0001	0.1132	2710	0.6	0.09%	/
	M_231	0.0004	0.0978	2710	0.6	0.41%	/
	M_331	0.0017	0.0921	2710	0.6	1.81%	/
	M_431	0.0000	0.1282	2710	0.6	0.00%	/
Layer 2	M_112	0.0002	0.1556	2710	0.6	0.13%	/
	M_212	0.0122	0.1055	2710	0.6	10.37%	100.0%
	M_312	0.0160	0.1029	2710	0.6	13.46%	100.0%
	M_412	0.0004	0.1360	2710	0.6	0.29%	/
	M_122	0.0000	0.0944	2710	0.6	0.00%	/
	M_222	0.0988	0.0793	2710	0.6	55.47%	100.0%
	M_322	0.0780	0.0520	2710	0.6	60.00%	100.0%
	M_422	0.0016	0.0860	2710	0.6	1.83%	/
	M_132	0.0001	0.1021	2710	0.6	0.10%	/
	M_232	0.0191	0.1330	2710	0.6	12.56%	100.0%
	M_332	0.0176	0.0945	2710	0.6	15.70%	100.0%
	M_432	0.0002	0.1053	2710	0.6	0.19%	/
Layer 3	M_113	0.0130	0.1515	2710	0.6	7.90%	100.0%
	M_213	0.0544	0.0853	2710	0.6	38.94%	100.0%
	M_313	0.0479	0.0735	2710	0.6	39.46%	100.0%
	M_413	0.0279	0.1355	2710	0.6	17.07%	100.0%
	M_123	0.0161	0.0871	2710	0.6	15.60%	100.0%
	M_223	0.1113	0.0673	2710	0.6	62.32%	100.0%
	M_323	0.1036	0.0684	2710	0.6	60.23%	100.0%
	M_423	0.0487	0.0789	2710	0.6	38.17%	100.0%
	M_133	0.0035	0.1510	2710	0.6	2.27%	100.0%
	M_233	0.0672	0.1455	2710	0.6	31.59%	100.0%
	M_333	0.0558	0.1130	2710	0.6	33.06%	100.0%
	M_433	0.0136	0.1380	2710	0.6	8.97%	100.0%

Case 2	Blocks	M_{wr}(kg)	$M_{paste.dried}$(kg)	ρ_s (kg/m^3)	e_f	C	S
Layer1	M_111	0.0092	0.1347	2710	0.6	6.4%	3085.8%
	M_211	0.0846	0.0679	2710	0.6	55.5%	169.2%
	M_311	0.0791	0.0537	2710	0.6	59.6%	143.1%
	M_411	0.0169	0.1186	2710	0.6	12.5%	1479.1%
	M_121	0.0364	0.1082	2710	0.6	25.2%	626.5%
	M_221	0.1200	0.0000	2710	0.6	100.0%	0.0%
	M_321	0.1290	0.0000	2710	0.6	100.0%	0.0%

	M_421	0.0326	0.1170	2710	0.6	21.8%	756.4%
	M_131	0.0054	0.1333	2710	0.6	3.9%	5202.7%
	M_231	0.0891	0.0672	2710	0.6	57.0%	159.0%
	M_331	0.0943	0.0600	2710	0.6	61.1%	134.2%
	M_431	0.0072	0.1615	2710	0.6	4.3%	4727.5%
Layer 2	M_112	0.0000	0.1346	2710	0.6	0.0%	/
	M_212	0.0101	0.1297	2710	0.6	7.2%	100.0%
	M_312	0.0044	0.1273	2710	0.6	3.3%	/
	M_412	0.0000	0.1532	2710	0.6	0.0%	/
	M_122	0.0023	0.1588	2710	0.6	1.4%	/
	M_222	0.0707	0.0829	2710	0.6	46.0%	100.0%
	M_322	0.0716	0.0869	2710	0.6	45.2%	100.0%
	M_422	0.0038	0.1315	2710	0.6	2.8%	/
	M_132	0.0000	0.1457	2710	0.6	0.0%	/
	M_232	0.0143	0.1602	2710	0.6	8.2%	100.0%
	M_332	0.0056	0.1407	2710	0.6	3.8%	/
	M_432	0.0000	0.1495	2710	0.6	0.0%	/
Layer 3	M_113	0.0000	0.1380	2710	0.6	0.0%	/
	M_213	0.0002	0.1731	2710	0.6	0.1%	/
	M_313	0.0025	0.1164	2710	0.6	2.1%	/
	M_413	0.0000	0.1161	2710	0.6	0.0%	/
	M_123	0.0000	0.1390	2710	0.6	0.0%	/
	M_223	0.0367	0.1055	2710	0.6	25.8%	100.0%
	M_323	0.0347	0.0811	2710	0.6	30.0%	100.0%
	M_423	0.0000	0.1376	2710	0.6	0.0%	/
	M_133	0.0000	0.1384	2710	0.6	0.0%	/
	M_233	0.0017	0.1361	2710	0.6	1.2%	/
	M_333	0.0017	0.1308	2710	0.6	1.3%	/
	M_433	0.0000	0.0985	2710	0.6	0.0%	/

Case 3	Blocks	M_{wr}(kg)	$M_{paste.dried}$(kg)	ρ_s (kg/m^3)	e_f	C	S
Layer1	M_111	0.0169	0.1341	2710	0.6	11.19%	1672.4%
	M_211	0.1398	0.0814	2710	0.6	63.20%	122.7%
	M_311	0.1399	0.0833	2710	0.6	62.67%	125.5%
	M_411	0.0138	0.1229	2710	0.6	10.10%	1877.0%
	M_121	0.0351	0.0977	2710	0.6	26.43%	586.6%
	M_221	0.1591	0.0000	2710	0.6	100.00%	0.0%
	M_321	0.1555	0.0000	2710	0.6	100.00%	0.0%
	M_421	0.0274	0.1038	2710	0.6	20.88%	798.4%
	M_131	0.0123	0.1398	2710	0.6	8.09%	2395.5%
	M_231	0.1399	0.0875	2710	0.6	61.51%	131.9%

	M_331	0.1315	0.0887	2710	0.6	59.72%	142.2%
	M_431	0.0116	0.1462	2710	0.6	7.35%	2656.3%
Layer 2	M_112	0.0000	0.1532	2710	0.6	0.00%	/
	M_212	0.0000	0.1334	2710	0.6	0.00%	/
	M_312	0.0000	0.1196	2710	0.6	0.00%	/
	M_412	0.0000	0.1493	2710	0.6	0.00%	/
	M_122	0.0000	0.1224	2710	0.6	0.00%	/
	M_222	0.0133	0.0895	2710	0.6	12.94%	100.0%
	M_322	0.0193	0.0783	2710	0.6	19.77%	100.0%
	M_422	0.0000	0.1515	2710	0.6	0.00%	/
	M_132	0.0000	0.1191	2710	0.6	0.00%	/
	M_232	0.0000	0.1318	2710	0.6	0.00%	/
	M_332	0.0000	0.1291	2710	0.6	0.00%	/
	M_432	0.0000	0.1391	2710	0.6	0.00%	/
Layer 3	M_113	0.0000	0.1417	2710	0.6	0.00%	/
	M_213	0.0000	0.1319	2710	0.6	0.00%	/
	M_313	0.0000	0.1323	2710	0.6	0.00%	/
	M_413	0.0000	0.1314	2710	0.6	0.00%	/
	M_123	0.0000	0.1445	2710	0.6	0.00%	/
	M_223	0.0000	0.1320	2710	0.6	0.00%	/
	M_323	0.0000	0.1120	2710	0.6	0.00%	/
	M_423	0.0000	0.1274	2710	0.6	0.00%	/
	M_133	0.0000	0.1344	2710	0.6	0.00%	/
	M_233	0.0000	0.1323	2710	0.6	0.00%	/
	M_333	0.0000	0.1402	2710	0.6	0.00%	/
	M_433	0.0000	0.1479	2710	0.6	0.00%	/

Case 4	Blocks	M_{wr}(kg)	$M_{paste.dried}$(kg)	ρ_s (kg/m^3)	e_f	*C*	*S*
Layer1	M_111	0.0034	0.1445	2710	0.6	2.30%	/
	M_211	0.0232	0.0908	2710	0.6	20.35%	806.1%
	M_311	0.0230	0.0916	2710	0.6	20.07%	820.2%
	M_411	0.0066	0.1199	2710	0.6	5.22%	/
	M_121	0.0125	0.1276	2710	0.6	8.92%	2102.4%
	M_221	0.1380	0.0133	2710	0.6	91.21%	19.8%
	M_321	0.1236	0.0074	2710	0.6	94.35%	12.3%
	M_421	0.0189	0.1276	2710	0.6	12.90%	1390.5%
	M_131	0.0012	0.1515	2710	0.6	0.79%	/
	M_231	0.0202	0.0815	2710	0.6	19.86%	831.0%
	M_331	0.0170	0.0710	2710	0.6	19.32%	860.2%
	M_431	0.0023	0.1447	2710	0.6	1.56%	/
Layer 2	M_112	0.0000	0.1416	2710	0.6	0.00%	/

	M_212	0.0082	0.1218	2710	0.6	6.31%	100.0%
	M_312	0.0253	0.1142	2710	0.6	18.14%	100.0%
	M_412	0.0000	0.1394	2710	0.6	0.00%	/
	M_122	0.0000	0.1181	2710	0.6	0.00%	/
	M_222	0.0646	0.0646	2710	0.6	50.00%	100.0%
	M_322	0.0685	0.0590	2710	0.6	53.73%	100.0%
	M_422	0.0049	0.1349	2710	0.6	3.51%	/
	M_132	0.0000	0.1194	2710	0.6	0.00%	/
	M_232	0.0169	0.1110	2710	0.6	13.21%	100.0%
	M_332	0.0117	0.1117	2710	0.6	9.48%	100.0%
	M_432	0.0000	0.0950	2710	0.6	0.00%	/
Layer 3	M_113	0.0000	0.1448	2710	0.6	0.00%	/
	M_213	0.0046	0.1368	2710	0.6	3.25%	/
	M_313	0.0108	0.1383	2710	0.6	7.24%	100.0%
	M_413	0.0000	0.1655	2710	0.6	0.00%	/
	M_123	0.0022	0.1449	2710	0.6	1.50%	/
	M_223	0.0976	0.0869	2710	0.6	52.90%	100.0%
	M_323	0.0822	0.0821	2710	0.6	50.03%	100.0%
	M_423	0.0010	0.1472	2710	0.6	0.67%	/
	M_133	0.0000	0.1691	2710	0.6	0.00%	/
	M_233	0.0336	0.1399	2710	0.6	19.37%	100.0%
	M_333	0.0255	0.1418	2710	0.6	15.24%	100.0%
	M_433	0.0000	0.1584	2710	0.6	0.00%	/

Case 5	Blocks	M_{wr}(kg)	$M_{paste.dried}$(kg)	ρ_s (kg/m^3)	e_f	C	S
Layer1	M_111	0.0042	0.1258	2710	0.6	3.23%	/
	M_211	0.0395	0.0751	2710	0.6	34.47%	391.6%
	M_311	0.0375	0.0627	2710	0.6	37.43%	344.4%
	M_411	0.0046	0.1236	2710	0.6	3.59%	/
	M_121	0.0116	0.1125	2710	0.6	9.35%	100%
	M_221	0.0855	0.0169	2710	0.6	83.50%	40.7%
	M_321	0.0841	0.0127	2710	0.6	86.88%	31.1%
	M_421	0.0101	0.0996	2710	0.6	9.21%	100%
	M_131	0.0000	0.1181	2710	0.6	0.00%	/
	M_231	0.0326	0.1105	2710	0.6	22.78%	698.1%
	M_331	0.0247	0.1062	2710	0.6	18.87%	885.5%
	M_431	0.0009	0.1447	2710	0.6	0.62%	/
Layer 2	M_112	0.0000	0.1339	2710	0.6	0.00%	/
	M_212	0.0342	0.1083	2710	0.6	24.00%	100.0%
	M_312	0.0454	0.1071	2710	0.6	29.77%	100.0%
	M_412	0.0022	0.1420	2710	0.6	1.53%	/

	M_122	0.0078	0.1087	2710	0.6	6.70%	/
	M_222	0.0958	0.0371	2710	0.6	72.08%	80%
	M_322	0.0950	0.0400	2710	0.6	70.37%	86.7%
	M_422	0.0014	0.1336	2710	0.6	1.04%	/
	M_132	0.0000	0.1157	2710	0.6	0.00%	/
	M_232	0.0352	0.1299	2710	0.6	21.32%	100.0%
	M_332	0.0380	0.1338	2710	0.6	22.12%	100.0%
	M_432	0.0000	0.1121	2710	0.6	0.00%	/
Layer 3	M_113	0.0000	0.1591	2710	0.6	0.00%	/
	M_213	0.0103	0.1309	2710	0.6	7.29%	100%
	M_313	0.0215	0.1337	2710	0.6	13.85%	100%
	M_413	0.0000	0.1704	2710	0.6	0.00%	/
	M_123	0.0000	0.1535	2710	0.6	0.00%	/
	M_223	0.0787	0.0894	2710	0.6	46.82%	100%
	M_323	0.0768	0.0821	2710	0.6	48.33%	100%
	M_423	0.0104	0.1518	2710	0.6	6.41%	100%
	M_133	0.0000	0.1490	2710	0.6	0.00%	/
	M_233	0.0317	0.1677	2710	0.6	15.90%	100%
	M_333	0.0320	0.1354	2710	0.6	19.12%	100%
	M_433	0.0000	0.1678	2710	0.6	0.00%	/

Case 6	Blocks	M_{wr}(kg)	$M_{paste.dried}$(kg)	ρ_s (kg/m^3)	e_f	C	S
Layer1	M_111	0.0034	0.1170	2710	0.6	2.82%	/
	M_211	0.0354	0.0669	2710	0.6	34.60%	389.2%
	M_311	0.0379	0.0714	2710	0.6	34.68%	388.0%
	M_411	0.0034	0.1110	2710	0.6	2.97%	/
	M_121	0.0054	0.1007	2710	0.6	5.09%	/
	M_221	0.1200	0.0283	2710	0.6	80.92%	48.6%
	M_321	0.0880	0.0209	2710	0.6	80.81%	48.9%
	M_421	0.0052	0.1150	2710	0.6	4.33%	/
	M_131	0.0030	0.1191	2710	0.6	2.46%	/
	M_231	0.0444	0.0699	2710	0.6	38.85%	324.2%
	M_331	0.0485	0.0691	2710	0.6	41.24%	293.4%
	M_431	0.0064	0.1512	2710	0.6	4.06%	/
Layer 2	M_112	0.0000	0.1404	2710	0.6	0.00%	/
	M_212	0.0044	0.1236	2710	0.6	3.44%	/
	M_312	0.0063	0.1316	2710	0.6	4.57%	/
	M_412	0.0000	0.1423	2710	0.6	0.00%	/
	M_122	0.0001	0.1199	2710	0.6	0.08%	/
	M_222	0.0650	0.0628	2710	0.6	50.86%	100%
	M_322	0.0670	0.0666	2710	0.6	50.15%	100%

	M_422	0.0038	0.1239	2710	0.6	2.98%	/
	M_132	0.0000	0.1187	2710	0.6	0.00%	/
	M_232	0.0017	0.1284	2710	0.6	1.31%	/
	M_332	0.0026	0.1130	2710	0.6	2.25%	/
	M_432	0.0000	0.1166	2710	0.6	0.00%	/
Layer 3	M_113	0.0017	0.1704	2710	0.6	0.99%	/
	M_213	0.0380	0.1365	2710	0.6	21.78%	100.0%
	M_313	0.0454	0.1634	2710	0.6	21.74%	100.0%
	M_413	0.0015	0.1928	2710	0.6	0.77%	/
	M_123	0.0069	0.1523	2710	0.6	4.33%	/
	M_223	0.1161	0.1028	2710	0.6	53.04%	100.0%
	M_323	0.1200	0.1197	2710	0.6	50.06%	100.0%
	M_423	0.0052	0.1698	2710	0.6	2.97%	/
	M_133	0.0050	0.1457	2710	0.6	3.32%	/
	M_233	0.0413	0.1379	2710	0.6	23.05%	100.0%
	M_333	0.0408	0.1611	2710	0.6	20.21%	100.0%
	M_433	0.0002	0.1874	2710	0.6	0.11%	/

Case 7	Blocks	M_{wr}(kg)	$M_{paste.dried}$(kg)	ρ_s (kg/m^3)	e_f	C	S
Layer1	M_111	0.0008	0.1563	2710	0.6	0.51%	/
	M_211	0.0027	0.1252	2710	0.6	2.11%	/
	M_311	0.0034	0.0901	2710	0.6	3.64%	/
	M_411	0.0027	0.1387	2710	0.6	1.91%	/
	M_121	0.0003	0.1382	2710	0.6	0.22%	/
	M_221	0.0327	0.1332	2710	0.6	19.71%	100%
	M_321	0.0300	0.1163	2710	0.6	20.51%	100%
	M_421	0.0008	0.0980	2710	0.6	0.81%	/
	M_131	0.0001	0.1205	2710	0.6	0.08%	/
	M_231	0.0002	0.1192	2710	0.6	0.17%	/
	M_331	0.0001	0.1038	2710	0.6	0.10%	/
	M_431	0.0001	0.1172	2710	0.6	0.09%	/
Layer 2	M_112	0.0240	0.1011	2710	0.6	19.18%	/
	M_212	0.0165	0.0970	2710	0.6	14.54%	100.0%
	M_312	0.0215	0.0948	2710	0.6	18.49%	100.0%
	M_412	0.0248	0.1231	2710	0.6	16.77%	100.0%
	M_122	0.0067	0.1008	2710	0.6	6.23%	100.0%
	M_222	0.0535	0.0970	2710	0.6	35.55%	100.0%
	M_322	0.0544	0.0948	2710	0.6	36.46%	100.0%
	M_422	0.0121	0.1422	2710	0.6	7.84%	100.0%
	M_132	0.0162	0.1238	2710	0.6	11.57%	100.0%
	M_232	0.0135	0.1162	2710	0.6	10.41%	100.0%

	M_332	0.0200	0.1148	2710	0.6	14.84%	100.0%
	M_432	0.0220	0.1204	2710	0.6	15.45%	100.0%
Layer 3	M_113	0.0201	0.1250	2710	0.6	13.85%	100.0%
	M_213	0.0176	0.0768	2710	0.6	18.64%	100.0%
	M_313	0.0167	0.0821	2710	0.6	16.90%	100.0%
	M_413	0.0281	0.1421	2710	0.6	16.51%	100.0%
	M_123	0.0269	0.1137	2710	0.6	19.13%	100.0%
	M_223	0.2011	0.1134	2710	0.6	63.94%	100.0%
	M_323	0.1810	0.1021	2710	0.6	63.94%	100.0%
	M_423	0.0234	0.1341	2710	0.6	14.86%	100.0%
	M_133	0.0300	0.2235	2710	0.6	11.83%	100.0%
	M_233	0.0185	0.1118	2710	0.6	14.20%	100.0%
	M_333	0.0358	0.1671	2710	0.6	17.64%	100.0%
	M_433	0.0225	0.1996	2710	0.6	10.13%	100.0%

Appendix II: Estimation of the mass of pure paste backfill in the blocks around the interfaces

In the tests, the mixtures were cut into small blocks with the same size. It was noted that the small blocks along the interfaces between waste rocks and paste backfill are too large, as shown in Fig. A1. Pure paste backfill (not mixed with any waste rocks) outside of interfaces were artificially added to the parts of mixture, resulting in the mass and portion of mixture inside the interfaces were diluted. Subsequently, the solids contents by mass of waste rocks *C* and the mixing degree *S* based on the direct measurements and calculations presented in Table A1 of Appendix I can be very inaccurate, especially around the interfaces between the waste rock and paste backfill.

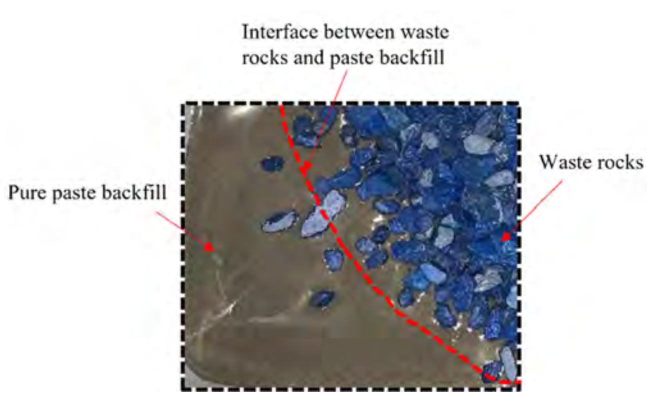

Fig. A1 Photo of a small block along the interface between waste rocks and paste backfill

In this study, corrections were made by excluding the mass of pure paste backfill $M'_{paste.dried}$, estimated based on observation of pictures, as shown in Fig. A2. The solids contents by mass of waste rocks and the mixing degree of the mixture based on these corrections are presented in Table A2.

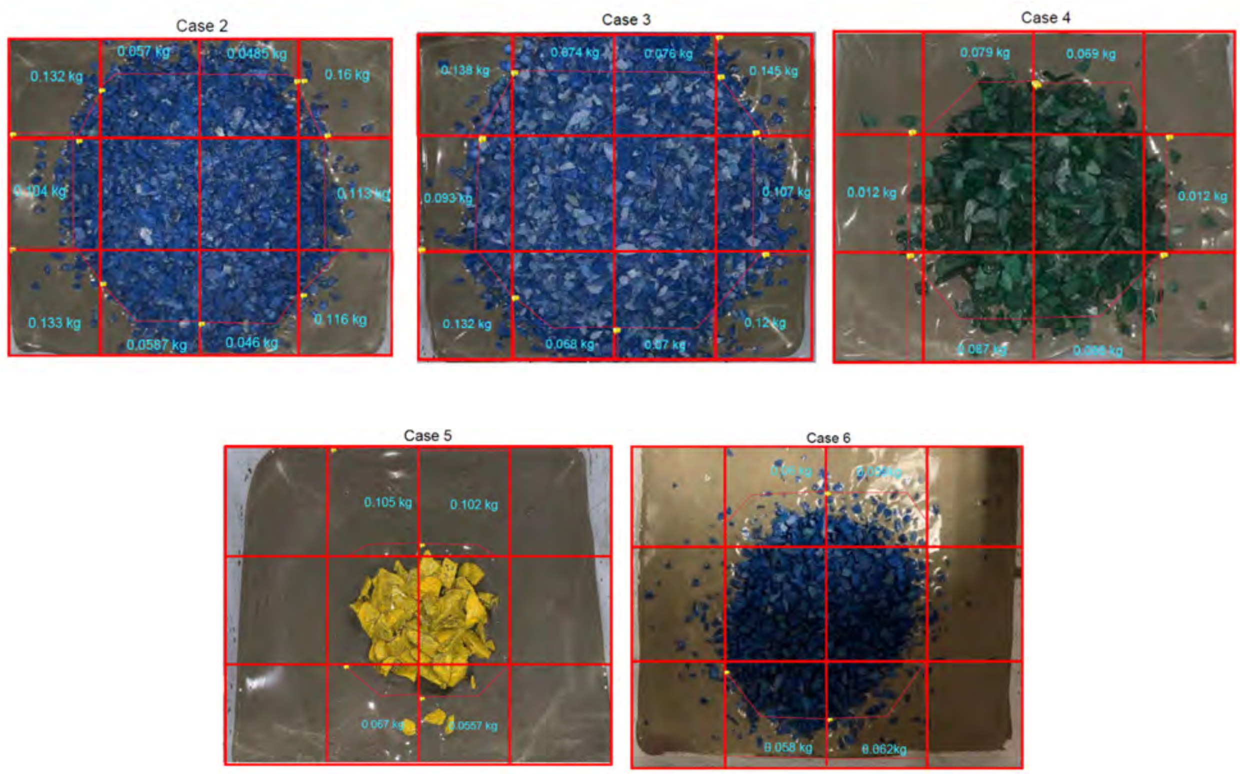

Fig. A2 Estimation of the mass of pure paste backfill in each block at layer 1

Table A2 Corrections of the solids content by mass of waste rocks C and mixing degree S of the blocks

Case 2	Blocks	M'_{paste}(kg)	$M'_{paste.dried}$(kg)	$M_{paste.dried}$(kg)	C	S
Layer 1	M_111	0.185	0.1338	0.0009	91.26%	20%
	M_211	0.081	0.0587	0.0092	90.23%	23%
	M_311	0.063	0.0460	0.0077	91.10%	21%
	M_411	0.161	0.1169	0.0017	90.67%	22%
	M_121	0.144	0.1047	0.0035	91.24%	20%
	M_421	0.157	0.1139	0.0031	91.31%	20%

	M_131	0.183	0.1328	0.0005	91.49%	20%
	M_231	0.080	0.0577	0.0095	90.38%	22%
	M_331	0.067	0.0485	0.0115	89.14%	26%
	M_431	0.222	0.1606	0.0009	89.26%	25%

Case 3	Blocks	M'_{paste}(kg)	$M'_{paste.dried}$(kg)	$M_{paste.dried}$(kg)	*C*	*S*
Layer 1	M_111	0.176	0.1320	0.0021	89.10%	26%
	M_211	0.091	0.0682	0.0132	91.35%	20%
	M_311	0.094	0.0703	0.0130	91.50%	20%
	M_411	0.162	0.1213	0.0016	89.60%	24%
	M_121	0.125	0.0939	0.0038	90.29%	23%
	M_421	0.134	0.1007	0.0031	89.80%	24%
	M_131	0.184	0.1384	0.0014	89.56%	25%
	M_231	0.099	0.0745	0.0130	91.49%	20%
	M_331	0.102	0.0763	0.0124	91.40%	20%
	M_431	0.193	0.1450	0.0012	90.39%	22%

Case 4	Blocks	M'_{paste}(kg)	$M'_{paste.dried}$(kg)	$M_{paste.dried}$(kg)	*C*	*S*
Layer 1	M_211	0.121	0.0879	0.0029	88.72%	26%
	M_311	0.122	0.0888	0.0028	89.22%	25%
	M_121	0.174	0.1262	0.0014	89.65%	24%
	M_421	0.173	0.1251	0.0025	88.47%	27%
	M_231	0.109	0.0792	0.0023	89.65%	24%
	M_331	0.095	0.0690	0.0020	89.25%	25%

Case 5	Blocks	M'_{paste}(kg)	$M'_{paste.dried}$(kg)	$M_{paste.dried}$(kg)	*C*	*S*
Layer 1	M_211	0.094	0.0679	0.0072	84.64%	37%
	M_311	0.077	0.0557	0.0070	84.22%	39%
	M_231	0.145	0.1052	0.0053	86.05%	33%
	M_331	0.141	0.1022	0.0040	85.92%	34%

Case 6	Blocks	M'_{paste}(kg)	$M'_{paste.dried}$(kg)	$M_{paste.dried}$(kg)	*C*	*S*
Layer 1	M_211	0.081	0.0587	0.0082	81.26%	47%
	M_311	0.086	0.0626	0.0088	81.10%	48%

	M_231	0.083	0.0605	0.0094	82.57%	43%
	M_331	0.082	0.0598	0.0093	83.85%	40%

References

Aubertin, M, 2013, ‘Waste rock disposal to improve the geotechnical and geochemical stability of piles’, paper presented at the 23rd World Mining Congress (WMC 2013), Montréal, pp. 8.

Aubertin, M, Li, L, Arnoldi, S, Belem, T, Bussière, B, Benzaazoua, M & Simon, R 2003, ‘Interaction between backfill and rock mass in narrow stopes’, *Soil and rock America*, vol. 1, no. 2, pp. 1157-1164.

Béket Dalcé, J, Li, L & Yang, P 2019, ‘Experimental study of uniaxial compressive strength (UCS) distribution of hydraulic backfill associated with segregation’, *Minerals*, vol. 9, no. 3, pp. 147.

El Mkadmi, N, Aubertin, M & Li, L 2014, ‘Effect of drainage and sequential filling on the behaviour of backfill in mine stopes’, *Canadian Geotechnical Journal*, vol. 51, no. 1, pp. 1-15.

Hassani, F & Archibald, J 1998, *Mine Backfill*, Canadian Institute of Mining, Metallurgy and Petroleum, Montreal.

Henning, J, 2007. Evaluation of Long-Hole Mine Design Influences on Unplanned Ore Dilution.

Jaouhar, E M & Li, L 2019, ‘Effect of drainage and consolidation on the pore water pressures and total stresses within backfilled stopes and on barricades’, *Advances in Civil Engineering*, vol. 2019, pp. 1-19.

Jaouhar, E M, Li, L & Aubertin, M 2018, ‘An analytical solution for estimating the stresses in vertical backfilled stopes based on a circular arc distribution’, *Geomechanics and Engineering*, vol. 15, no. 3, pp. 889-898.

Keita, A M T, Jahanbakhshzadeh, A & Li, L 2021a, ‘Numerical analysis of the stability of arched sill mats made of cemented backfill’, *International Journal of Rock Mechanics and Mining Sciences*, vol. 140, no. 4, article 104667.

Keita, A M T, Jahanbakhshzadeh, A & Li, L 2021b, ‘Numerical analysis of the failure mechanisms of sill mats made of cemented backfill’, *International Journal of Geotechnical Engineering*, vol. 16, no. 7, pp. 802-814.

Kuganathan, K & Sheppard, I 2001, ‘A non-segregating ‘rocky paste fill’ (RPF) produced by co-disposal of cemented de-slimed tailings slurry and graded rockfill’, in D Stone (ed.), *Proceedings of the Seventh International Symposium on Mining with Backfill*, Society for Mining, Metallurgy and Exploration, Englewood, pp. 27–41.

Lee, C & Gu, F 2017, ‘An examination of improvements in co-disposal of waste rock with backfill’, in A Wu & R Jewell (eds), *Paste 2017: Proceedings of the 20th International Seminar on Paste and Thickened Tailings*, University of Science and Technology Beijing, Beijing, pp. 338-345.

Li, L 2014a, ‘Analytical solution for determining the required strength of a side-exposed mine backfill containing a plug’, *Canadian Geotechnical Journal*, vol. 51, no. 5, pp. 508-519.

Li, L 2014b, ‘Generalized solution for mining backfill design’, *International Journal of Geomechanics*, vol. 14, no. 3, article 04014006.

Li, L & Aubertin, M 2012, ‘A modified solution to assess the required strength of exposed backfill in mine stopes’, *Canadian Geotechnical Journal*, vol. 49, no. 8, pp. 994-1002.

Li, L & Aubertin, M 2014, ‘An improved method to assess the required strength of cemented backfill in underground stopes with an open face’, *International Journal of Mining Science and Technology*, vol. 24, no. 4, pp. 549-558.

Li, L, Aubertin, M & Belem, T 2005, ‘Formulation of a three-dimensional analytical solution to evaluate stresses in backfilled vertical narrow openings’, *Canadian Geotechnical Journal*, vol. 42, no. 6, pp. 1705-1717.

Li, L, Aubertin, M, Simon, R, Bussière, B & Belem, T 2003, ‘Modeling arching effects in narrow backfilled stopes with FLAC’, in R Brummer, P Andrieux, C Detournay & R Hart (eds), *Proceedings of 3rd international symposium on FLAC and FLAC3D numerical modelling in geomechanics*, A. A. Balkema, a member of Swets & Zeitlinger Publishers, Sudbury, pp. 211–219.

Liu, G, Li, L, Yang, X & Guo, L 2017a, ‘Numerical analysis of stress distribution in backfilled stopes considering interfaces between the backfill and rock walls’, *International Journal of Geomechanics*, vol. 17, no. 2, article 06016014.

Liu, G, Li, L, Yang, X & Guo, L 2018, ‘Required strength estimation of a cemented backfill with the front wall exposed and back wall pressured’, *International Journal of Mining and Mineral Engineering*, vol. 9, no. 1, pp. 1-20.

Liu, G, Li, L, Yao, M, Landry, D, Malek, F, Yang, X & Guo, L 2017b, ‘An investigation of the uniaxial compressive strength of a cemented hydraulic backfill made of alluvial sand’, *Minerals*, vol. 7, no. 1, pp. 4.

Pagé, P, Li, L, Yang, P & Simon, R 2019, ‘Numerical investigation of the stability of a base-exposed sill mat made of cemented backfill’, *International Journal of Rock Mechanics and Mining Sciences*, vol. 114, no. 2, pp. 195-207.

Potvin, Y, Thomas, E, & Fourie, A 2005, *Handbook on Mine Fill*, Australian Centre for Geomechanics, Perth.

Qin, J, Zheng, J & Li, L 2021a, ‘An analytical solution to estimate the settlement of tailings or backfill slurry by considering the sedimentation and consolidation’, *International Journal of Mining Science and Technology*, vol. 31, no. 3, pp. 463-471.

Qin, J, Zheng, J & Li, L 2021b, ‘Experimental study of the shrinkage behaviour of cemented paste backfill’, *Journal of Rock Mechanics and Geotechnical Engineering*, vol. 13, no. 3, pp. 545-554.

Qiu, H, Zhang, F, Liu, L, H, D & T, B 2020, ‘Influencing factors on strength of waste rock tailing cemented backfill’. *Geofluids*, pp. 1-7.

Qiu, H, Zhang, F, Sun, W, Liu, L, Zhao, Y & Huan, C 2022, ‘Experimental study on strength and permeability characteristics of cemented rock-tailings backfill’. *Frontiers in Earth Science*.

Saleh-Mbemba, F., Aubertin, M., Mbonimpa, M 2016, ‘Experimental characterization of the shrinkage and water retention behaviour of tailings from hard rock mines’, *Geotechnical and Geological Engineering*, vol. 34, pp. 251–266.

Sobhi, MA & Li, L 2017, ‘Numerical investigation of the stresses in backfilled stopes overlying a sill mat’, *Journal of Rock Mechanics and Geotechnical Engineering*, vol. 9, no. 3, pp. 490-501.

Sobhi, MA, Li, L & Aubertin, M 2017, ‘Numerical investigation of earth pressure coefficient along central line of backfilled stopes’, *Canadian Geotechnical Journal*, vol. 54, no. 1, pp. 138-145.

Veenstra, RL & Grobler, JJ 2021, ‘Paste-waste design and implementation at Newmont Goldcorp’s Tanami Operation’, in F Hassani, J Palarski, V Sokoła-Szewioła & G Strozik (eds), *Minefill 2020-2021: Proceedings of the 13th International Symposium on Mining with Backfill*, CRC Press, Katowice, pp. 382-397.

Wang, R & Li, L 2022, ‘Time-dependent stability analyses of side-exposed backfill considering creep of surrounding rock mass’, *Rock Mechanics and Rock Engineering*, vol. 55, no. 4, pp. 2255-2279.

Wang, R, Zeng, F & Li, L 2021a, ‘Applicability of constitutive models to describing the compressibility of mining backfill: a comparative study’, *Processes*, vol. 9, no. 12, article 2139.

Wang, R, Zeng, F & Li, L 2021b, ‘Stability analyses of side-exposed backfill considering mine depth and extraction of adjacent stope’, *International Journal of Rock Mechanics and Mining Sciences*, vol. 142, no. 6, article 104735.

Wickland, BE & Wilson, GW 2005, ‘Self-weight consolidation of mixtures of mine waste rock and tailings’, *Canadian Geotechnical Journal*, vol. 42, no. 2, pp. 327-339.

Wilson, G 2001, ‘Co-disposal of tailings and waste rock’, *Geotechnical News*, vol. 19, no. 2, pp. 44-49.

Wilson, GW, Wickland, B & Miskolczi, J 2008, ‘Design and performance of paste rock systems for improved mine waste management’, in AB Fourie (ed.), *Rock Dumps 2008: Proceedings of the First International Seminar on the Management of Rock Dumps, Stockpiles and Heap Leach Pads*, Australian Centre for Geomechanics, Perth, pp. 107-116.

Yan, B, Zhu, W, Hou, C, Yilmaz, E, & Saadat, M 2020. ‘Characterization of early age behavior of cemented paste backfill through the magnitude and frequency spectrum of ultrasonic P-wave’, *Construction and Building Materials*, 249, 118733.

Yan, B, Jia, H, Yilmaz, E, Lai, X, Shan, P, & Hou, C 2022a. ‘Numerical investigation of creeping rockmass interaction with hardening and shrinking cemented paste backfill’, *Construction and Building Materials*, 340, 127639.

Yan, B, Jia, H, Yilmaz, E, Lai, X, Shan, P, & Hou, C 2022b. ‘Numerical study on microscale and macroscale strength behaviors of hardening cemented paste backfill’, *Construction and Building Materials*, 321, 126327.

Yang, P, Li, L & Aubertin, M 2018, ‘Theoretical and numerical analyses of earth pressure coefficient along the centreline of vertical openings with granular fills’, *Applied Sciences*, vol. 8, no. 10, article 1721.

Yang, P, Li, L, Aubertin, M, Brochu-Baekelmans, M & Ouellet, S 2017, ‘Stability analyses of waste rock barricades designed to retain paste backfill’, *International Journal of Geomechanics*, vol. 17, no. 3, article 04016079.

Zhai, Y, Yang, P & Li, L 2021, ‘Analytical solutions for the design of shotcreted waste rock barricades to retain slurried paste backfill’, *Construction and Building Materials*, vol. 307, article 124626.

Zheng, J & Li, L 2020, ‘Experimental study of the “short-term” pressures of uncemented paste backfill with different solid contents for barricade design’, *Journal of Cleaner Production*, vol. 275, article 123068.

Zheng, J, Li, L & Li, Y 2019, ‘Total and effective stresses in backfilled stopes during the fill placement on a pervious base for barricade design’, *Minerals*, vol. 9, no. 1, pp. 38.

Zheng, J, Li, L & Li, Y 2020a, ‘A solution to estimate the total and effective stresses in backfilled stopes with an impervious base during the filling operation of cohesionless backfill’, *International Journal for Numerical and Analytical Methods in Geomechanics*, vol. 44, no. 11, pp. 1570-1586.

Zheng, J, Li, L & Li, Y 2020b, ‘Solutions to estimate the excess PWP, settlement and volume of draining water after slurry deposition. Part I: impervious base’, *Environmental Earth Sciences*, vol. 79, no. 6, article 124 (2020).

Zheng, J, Li, L & Li, Y 2020c, ‘Solutions to estimate the excess PWP, settlement and volume of draining water after slurry deposition. Part II: pervious base’, *Environmental Earth Sciences*, vol. 79, no. 11, article 275 (2020).